Modelling and simulation of intensified absorber for post-combustion CO_2 capture using different mass transfer correlations

Atuman S. Joel, Meihong Wang*, Colin Ramshaw

Process\Energy Systems Engineering Group, School of Engineering, University of Hull, HU6 7RX, UK

**Corresponding author. Tel: +0044 (0)1482 466688; Fax: +0044 1482 466664; Email address: Meihong.Wang@hull.ac.uk*

ABSTRACT

This paper studied mass transfer in rotating packed bed (RPB) which has the potential to significantly reduce capital and operating costs in post-combustion CO_2 capture. To model intensified absorber, mass transfer correlations were implemented in visual FORTRAN and then were dynamically linked with Aspen Plus® rate-based model. Two sets of mass transfer correlations were studied and compared through model validations. The second set of correlations performed better at the MEA concentrations tested as compared with the first set of correlations. For insights into the design and operation of intensified absorber, process analysis were carried out, which indicates: (a) With fixed RPB equipment size and fixed lean MEA flow rate, CO_2 capture level decreases with increase in flue gas flow rate; (b) Higher lean MEA inlet temperature leads to higher CO_2 capture level. (c) At higher flue gas temperature (from 30 ^oC to 80 ^oC), the CO_2 capture level of the intensified absorber can be maintained. Compared with conventional absorber using packed columns, the insights obtained from this study are (1) Intensified absorber using RPB improves mass transfer significantly. (2) Cooling duty cost can be saved since higher lean MEA temperature can improve the performance of RPB and high flue gas temperature shows little or no effect on the performance of the RPB.

Keywords: *Post-combustion, CO_2 capture, Chemical Absorption, MEA solvent, Process Intensification (PI), Rotating Packed Bed (RPB), Process simulation,*

Introduction

Carbon dioxide (CO_2) emission has become crucial environmental concern in recent years because of its contribution to global warming. Combustion of coal and petroleum accounts for the majority of CO_2 emissions. Petroleum is mostly used as a transportation fuel for vehicles while coal is used mostly for electricity generation, for instance about 85.5% of coal is used for electricity generation in 2011 in the UK [1]. Moulijn *et al.* [2] stated that among the greenhouse gases, CO_2 contributes more than 60% to global warming. Atmospheric CO_2 concentration is close to 400 ppm which is higher than the pre-industrial level of about 300 ppm [3], this increased atmospheric concentrations of CO_2 affect the radiative balance of the Earth and, consequently, its temperature and other aspects of its climate.

In order to meet the set target of 50% emission reduction as compared to the level of 1990 as proposed by Intergovernmental panel on climate change (IPCC) [4], carbon capture and storage (CCS) is an important option for that to be achieved. The International Energy Agency (IEA) [5] identifies CCS as a significant and low-cost option in fighting climate change. The most matured CO_2 capture technology is post-combustion CO_2 capture (PCC) with chemical absorption as reported in Mac Dowell *et al.* [6] which is also believed to be a low-risk technology and promising near-term option for large-scale CO_2 capture.

Post-combustion CO_2 Capture for coal-fired power plants using conventional absorber has been reported by many authors. Dugas [7] carried out pilot plant study of post-combustion CO_2 capture in the context of fossil fuel-fired power plants. Lawal *et al.* [8,9,10] carried out dynamic modelling of CO_2 absorption for post-combustion capture in coal-fired power plants. In these studies, one of the identified challenges to the commercial roll out of the technology has been the large size of the packed columns needed. This translates to high capital and operating cost and unavoidable impact on electricity cost. Approaches such as heat integration, inter-cooling among others could reduce the operating cost slightly. However, they limit the plant flexibility and will make operation and control more difficult [11]. Process intensification (PI) has the potential to meet this challenge [12,13,14].

Nomenclature

A	gas-liquid interfacial area (m^2/m^3)
a	fibre diameter (m)
a_t	total specific surface area of packing (m^2/m^3)
c	mesh square opening (m)
D_L	diffusivity coefficient of liquid (m^2/s)
d_p	diameter of packing pore (m)

G	superficial gas velocity (m/s)
g_c	gravitational acceleration or acceleration due to centrifugal field (m^2/s)
g_o	characteristic acceleration value (100 m^2/s)
k_L	liquid phase mass transfer coefficient (m/s)
L	superficial liquid velocity (m/s)
Q_L	volumetric flow rate of liquid (m^3/s)
R	radial position (m)
T	temperature (K)
U	superficial flow velocity (m/s)
U_o	characteristic superficial flow velocity (1cm/s)
$y_{CO_{2,in}}$	Mole fraction of CO_2 in inlet stream
$y_{CO_{2,out}}$	Mole fraction of CO_2 in outlet stream
Z	axial height of the packing (m)

Greek letters

$\in_L$	liquid holdup
μ	Viscosity (Pa.s)
ρ_L	liquid density (kg/m^3)
ρ_G	gas density (kg/m^3)
σ	liquid surface tension (N/m)
σ_c	critical surface tension (N/m)
v_L	kinematic liquid viscosity (m^2/s)
v_G	kinematic gas viscosity (m^2/s)
ω	angular velocity (rad/s)

Dimensionless groups

Fr_L	liquid Froude number $(L^2 a_t / g_c)$
Gr_G	gas Grashof number $\left(d_p^3 g_c / v_G^2\right)$
Gr_L	liquid Grashof number $\left(d_p^3 g_c / v_L^2\right)$
Re_G	gas Reynolds number $(G/a_t v_G)$
Re_L	liquid Reynolds number $(L/a_t v_L)$
Sc_L	liquid Schmidt number (v_L/D_L)
We_L	liquid Webber number $(L^2 \rho_L / a_t \sigma)$

φ $c^2/(d+c)^2$

1.1 Motivation

Over 8,000 tonnes of CO_2 per day will be released from 500 MWe supercritical coal fired power plant operating at 46% efficiency (LHV basis) [15]. This big volume of flue gas will result in the use of high amount of solvent and big size of packed columns if conventional technology is to be applied. Lawal *et al.* [16] reported dynamic modelling study of a 500MWe sub-critical coal-fired power plant using the conventional packed column. From the analysis, two absorbers of 17m in packing height and 9m in diameter will be needed to separate CO_2 from the flue gas. These huge conventional packed columns will mean higher capital and operating costs. This could increase electricity costs by over 50% and has been a major impediment to commercializing the technology.

1.3 Novel contributions of the paper

There are two novel aspects in this paper: (a) steady state validation of the intensified absorber is performed, where comparison is made by using two different sets of mass transfer correlations and the results indicated that Set 2 correlations give better predictions at higher (i.e. 75 wt%) and lower (i.e. 56 wt%) MEA concentration than Set 1. (b) With the models developed using Set 2 correlations and validated, process analysis of the intensified absorber with RPB involving different process scenarios were carried out to gain insights for process design and operation. These process scenarios are: (i) when the RPB absorber size is fixed and lean MEA flow rate is fixed, the impact of flue gas flow rate on CO_2 capture level was explored;. (ii) The effect of higher lean MEA temperature on CO_2 capture level for RPB absorber was explored; (iii) the effect of higher flue gas temperature on CO_2 capture level was explored. The results indicate higher lean-MEA temperature increases CO_2 capture level and at higher flue gas temperature, CO_2 capture level can be maintained. These results indicate that cooling duty for lean MEA and flue gas can be greatly reduced.

Comparison between this paper and Joel *et al.* [17], there are three main differences: (a) In Joel *et al.* [17] only Set 1 correlations were used while in this paper Set 1 and Set 2 correlations were studied and implemented. (b) Process analysis was done using Set 1 correlations in Joel *et al.* [17] while Set 2 correlations were used in this paper. (c) Process scenarios considered in Joel *et al.* [17] were effect of lean MEA concentration, effect of rotating speed, effect of lean MEA temperature on CO_2 capture level and temperature bulge analysis in RPB. While in this paper process scenarios considered are: Effect of flue gas flow rate, effect of lean MEA temperature and effect of flue gas temperature on CO_2 capture level.

1 Model Development

In a typical RPB absorber, flue gas and lean-MEA solvent were contacted counter-currently. To model intensified absorber with RPB, mass transfer correlations inside the Aspen Plus® rate-based absorber model were modified using subroutines written in Intel® visual FORTRAN. The first set of correlations studied include liquid phase mass transfer coefficient given by Tung and Mah [18], gas phase mass transfer coefficient given by Onda *et al.* [19], Interfacial area correlation modified by updating the gravity term in the equation with centrifugal acceleration given by Onda *et al.* [19], and Liquid holdup evaluated using Burns *et al.* [20] correlation. The second set of correlations include: liquid phase mass transfer coefficient given by Chen *et al.* [21], gas-phase mass transfer coefficient given by Chen [22], interfacial area correlation estimated by Luo *et al.* [23] and Liquid hold-up correlation given by Burns *et al.* [20].

Aspen Plus® rate-based absorber model and visual FORTRAN were dynamically linked to model RPB absorber. Electrolyte Non-Random-Two-Liquid (ElecNRTL) activity coefficient model is used for physical properties calculation. The coefficient of equilibrium constant and equilibrium reactions which are assumed to occur in the liquid film are found in Biliyok *et al.* [24]. Kinetics reactions equations and parameters are obtained in AspenTech [25]. Process parameters can be found in Jassim *et al.* [26]

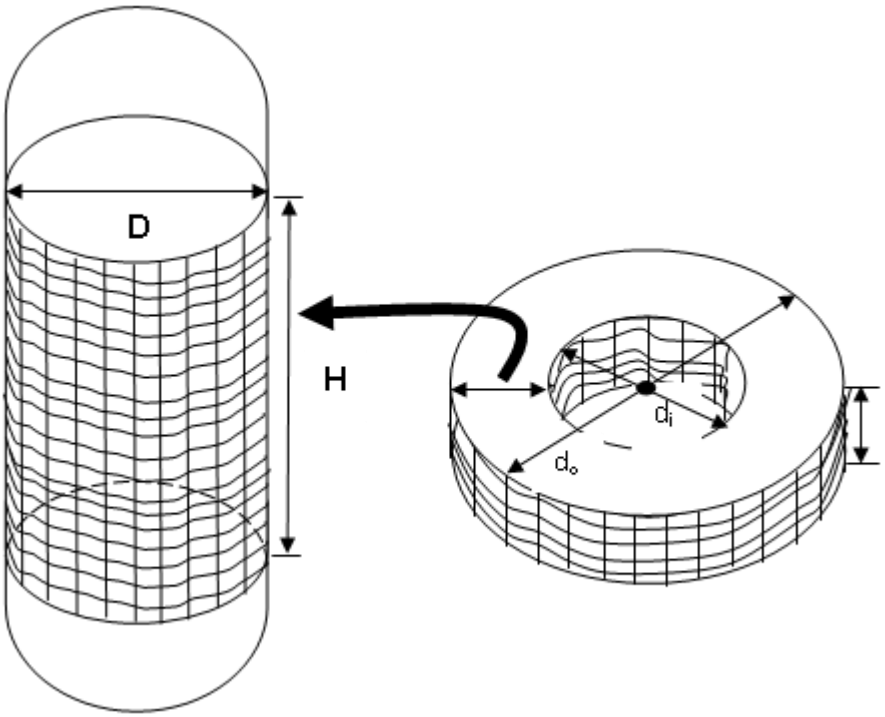

Figure 1: Figure showing dimension relation between RPB and Conventional absorber

1.1 *Liquid phase mass transfer coefficient*

An expression was introduced by Tung and Mah [18] using the penetration model to describe the liquid mass transfer behaviour in the RPB.

$$\frac{k_L d_p}{D_L} = 0.919\left(\frac{a_t}{a}\right)^{1/3} Sc_L^{1/2} Re_L^{2/3} Gr_L^{1/6} \quad (1)$$

g_c in the Grashof number Gr_L is taken as $g_c = rw^2$ to account for the effect of rotation in the RPB absorber.
This correlation was developed without considering the Coriolis force or the effect of the packing geometry.

Chen *et al,* [21] developed liquid phase mass transfer correlation that put into consideration the end effect and packing geometry. The correlation was found to be valid for different sizes of the RPBs and for viscous Newtonian and non-Newtonian fluids.

$$\frac{k_L a d_p}{D_L a_t}\left(1 - 0.93\frac{V_o}{V_t} - 1.13\frac{V_i}{V_t}\right) = 0.35 Sc_L^{0.5} Re_L^{0.17} Gr_L^{0.3} We_L^{0.3} \left(\frac{a_t}{a_p'}\right)^{-0.5}\left(\frac{\sigma_c}{\sigma_w}\right)^{0.14} \quad (2)$$

1.2 *Gas phase mass transfer coefficient*

Onda *et al.* [19] correlation for calculating gas-side mass transfer coefficient was developed for conventional packed column. Sandilya *et al.* [27] suggested that the gas rotated like a solid body in the rotor because of the drag that was caused by the packing and that, consequently, the gas-side mass transfer coefficient should be similar to that in a conventional packed column.

$$k_G = 2.0(a_t D_G) Re_G^{0.7} Sc_G^{1/3} \left(a_t d_p\right)^{-2} \quad (3)$$

Chen [22] presented local gas-side mass transfer coefficient correlation using two-film theory for RPB.

$$\frac{k_G a}{D_G a_t^2}\left(1 - 0.9\frac{V_o}{V_t}\right) = 0.023 Re_G^{1.13} Re_L^{0.14} Gr_G^{0.31} We_L^{0.07}\left(\frac{a_t}{a_p'}\right)^{1.4} \quad (4)$$

1.3 *Total gas-liquid interfacial area*

Total gas-liquid interfacial area is calculated with the Onda *et al.* [19] correlation.

$$\frac{a}{a_t} = 1 - exp\left[-1.45\left(\frac{\sigma_c}{\sigma}\right)^{0.75} Re_L^{0.1} We_L^{0.2} Fr_L^{-0.05}\right] \quad (5)$$

Similarly, g_c in the Froude number Fr_L is taken as $g_c = rw^2$ to account for the effect of rotation in the RPB absorber.

Luo *et al.* [23] studied gas-liquid effective interfacial area in an RPB considering different types of packing, also taking into account the effect of fibre diameter and opening of the wire mesh.

$$\frac{a}{a_t} = 66510 Re_L^{-1.41} Fr_L^{-0.12} We_L^{1.21} \varphi^{-0.74} \quad (6)$$

1.4 *Liquid hold-up*

Liquid holdup correlation by Burns *et al.* [20] is given as:

$$\in_L = 0.039\left(\frac{g_c}{g_o}\right)^{-0.5}\left(\frac{U}{U_o}\right)^{0.6}\left(\frac{v}{v_o}\right)^{0.22} \quad (7)$$

$$g_o = 100\ m\ s^{-2}, \quad U_o = 1\ cm\ s^{-1}, \quad v_o = 1\ cS = 10^{-6}\ m^2\ s^{-1}$$

$$U = \frac{Q_L}{2\pi r Z} \quad (8)$$

1.5 *Modelling and simulation methodology*

The procedure used in this paper for modelling and simulation of the RPB is shown in **Figure 2**.

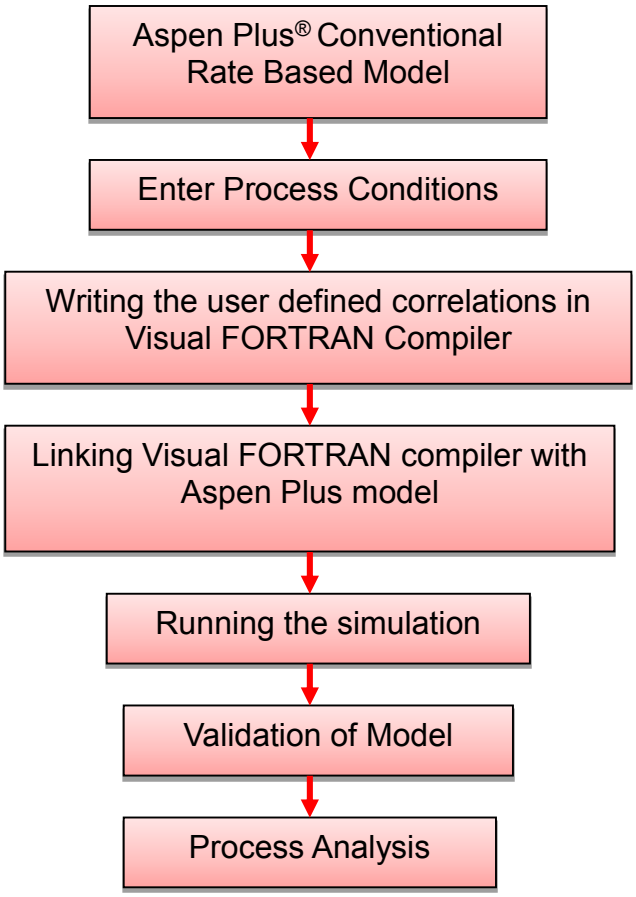

Figure 2 Methodology used in this paper

2 **Model Validation**

The experimental data used for model validation was obtained from Jassim *et al.* [26]. From their experiments, two lean-MEA concentration (average 55 wt% and 75 wt%) were selected so as to fall within a reasonable range of MEA concentration to minimize the problem of corrosion and maximize CO_2 absorption rate.

Two sets of correlations were used for the validation. The sets of correlations are presented in Table 1 and the input condition is shown in Table 2.

Table 1 Model correlation sets used for the modelling and simulations

Correlations	Set 1	Set 2
Liquid-phase mass transfer coefficient	Tung and Mah [18]	Chen *et al.* [21]
Gas-phase mass transfer coefficient	Onda *et al.* [19]	Chen, [22]
Interfacial area	Onda *et al.* [19]	Luo *et al.* [23]
Liquid hold-up	Burns *et al.* [20]	Burns *et al.*[20]

Table 2 Input process conditions for Run 1 to Run 4 [26]

Variable	Runs

	Run 1	Run 2	Run 3	Run 4
Rotor speed (RPM)	600	1000	600	1000
Lean temperature (^oC)	39.6	40.1	41	40.2
Lean pressure (atm.)	1	1	1	1
Flue gas flow rate (kmol/hr)	2.87	2.87	2.87	2.87
CO_2 composition in Flue gas (vol %)	4.71	4.48	4.40	4.29
Lean-MEA flow rate (kg/s)	0.66	0.66	0.66	0.66
Lean-MEA composition (wt %)				
H_2O	40.91	40.91	22.32	23.41
CO_2	3.09	3.09	2.68	2.59
MEA	56.00	56.00	75.00	74.00

Table 3 Simulation results with 2 different sets of correlations compared to the experimental data for Run 1 and Run 2

Variable	Run 1					Run 2				
	Expt.	Set 1	Error 1	Set 2	Error 2	Expt.	Set 1	Error 1	Set 2	Error 2
CO_2 loading of Lean MEA, (mol CO_2/mol MEA)	0.0772	0.0772		0.0772		0.0772	0.0772		0.0772	
CO_2 loading of Rich MEA, (mol CO_2/mol MEA)	0.0828	0.0827	0.1208	0.0829	0.1208	0.0828	0.0825	0.3623	0.0827	0.1208
Average Lean MEA/Rich MEA, (mol CO_2/mol MEA)	0.0800	0.0800	0.0000	0.0800	0.0000	0.0800	0.0799	0.1250	0.0801	0.1250
CO_2 capture level (%)	94.9	92.9	2.1075	96.72	1.9178	95.4	93.26	2.2432	96.95	1.6247

Table 4 Simulation results with 2 different sets of correlations compared to the experimental data for Run 3 and Run 4

Variable	Run 3					Run 4				
	Expt.	Set 1	Error 1	Set 2	Error 2	Expt.	Set 1	Error 1	Set 2	Error 2
CO_2 loading of Lean–MEA, (mol CO_2/mol MEA)	0.0492	0.0492		0.0492		0.0483	0.0483		0.0483	
CO_2 loading of Rich-MEA, (mol CO_2/mol MEA)	0.0531	0.0530	0.1883	0.0531	0.0000	0.0510	0.0521	2.1569	0.0524	2.7451
Average Lean-MEA/Rich-MEA, (mol CO_2/mol MEA)	0.0512	0.0511	0.1953	0.0512	0.0000	0.0497	0.0502	1.0060	0.0503	1.2072
CO_2 capture level (%)	98.20	93.28	5.0102	97.36	0.8554	97.50	93.57	4.0308	98.66	1.1897

Validation results were presented in terms of CO_2 capture level which is defined as:

$$\boldsymbol{CO_2 capture\ level}\ (\%) = \left(\frac{\boldsymbol{y_{CO_{2,in}}} - \boldsymbol{y_{CO_{2,out}}}}{\boldsymbol{y_{CO_{2,in}}}}\right) \times \mathbf{100} \qquad (\mathbf{9})$$

In **Table 3**, the model predictions were compared with experimental data for the two correlation sets in **Table 1** and for input conditions in **Table 2**. For **Run 1** (56 wt% MEA concentration and 600rpm rotor speed) the CO_2 capture level of **Set 1** correlation is 92.90 while that of **Set 2** is 96.36. For both sets of correlations, the model reasonably predicts the experimental data with prediction error less than 3%

In **Table 4**, the simulation predictions were compared to experimental data at the input conditions shown in **Table 2.** The error prediction of **Runs 3 and 4** using **Set 2** correlation gives better agreement with the experiment data, the reason for this could be from the liquid and gas phase mass transfer resistance where Chen et al. [21] and Chen [22] account for the effect of viscosity and packing geometry.

This results show that the model developed using Aspen Plus® rate-based absorber model modified for RPB with correlations implemented in visual FORTRAN is able to reasonably capture the behaviour of an RPB absorber. As a result, the model can be used to analyse typical RPB behaviour at different input conditions.

3 **Process Analysis**

In this section, the model developed and validated is used to analyse the process characteristics of the RPB absorber.

3.1 *Effect of Flue Gas Flow Rate on CO_2 Capture Level*

3.1.1 Justification for case study

In designing RPB, flue gas flow rate is an important parameter in determining the size of the absorption column, also for CO_2 emission target to be met this process analysis is necessary.

3.1.2 Setup of the case study

For this study, Set 2 of the correlations in Table 1 was used and the input conditions in Table 2 for Run 2 and Run 4 having constant rotor speed of 1000rpm were selected for the analysis. The RPB absorber size is fixed, as well as the lean MEA flow rate. The flue gas flow rate was varied from 0.02 kg/s to 1 kg/s.

3.1.3 Results and discussions

Figure 3 shows that for both Runs 2 and 4, CO_2 capture level decrease as the flue gas flow rate increases. This is associated with decrease in contact time (i.e. residence time) between the flue gas and liquid MEA solvent resulting in more CO_2 escaping the RPB without being captured. Also from Figure 3, it can be seen that whatever the MEA concentration of the solvent the trend is the same.

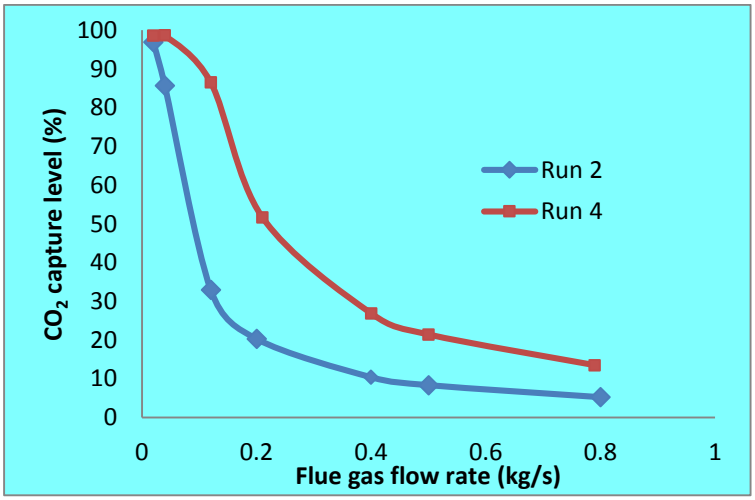

Figure 3 Effect of flue gas flow rate of CO_2 capture level

3.2 *Effect of Lean-MEA Temperature on CO_2 Capture Level*

3.2.1 Justification for case study

The study is performed to investigate the effect of lean MEA temperature on the performance of RPB absorber. In absorber with conventional packed column, the mass transfer decreases with temperature and chemical reaction increases with temperature [28]. Conventional absorber performance is already known to be hindered by increase in lean MEA temperature due to the possibility of temperature bulge within the absorber column [29]. Based on this, capture performance with lean MEA temperature should be studied for RPB absorbers.

3.2.2 Setup of the case study

Set 2 correlation is used in the implementation of this case study. Process conditions are shown in Table 5. Rotor speed of 1000 rpm, lean MEA flow rate of 0.66 kg/s and lean MEA temperature which is varied from 25 ^{o}C, 30 ^{o}C, 35 ^{o}C, 40 ^{o}C … to 80 ^{o}C at 55 wt% and 75 wt% lean MEA concentrations were used.

Table 5 Process Conditions for lean MEA temperature studies

Variable	**55 wt% MEA Con.**	**75 wt% MEA Con.**
Rotor speed (RPM)	1000	1000
Lean pressure (atm.)	1	1
Flue gas flow rate (kmol/hr)	2.87	2.87
Flue gas composition (vol %)		
H_2O	17.1	17.1
CO_2	4.4	4.4
N_2	78.5	78.5
Lean-MEA flow rate (kg/s)	0.66	0.66
Lean-MEA composition (wt %)		
H_2O	41.03	22.32
CO_2	3.97	2.68
MEA	55.00	75.00

3.2.3 Results and discussions

Figure 4 shows the effect of varying lean MEA temperature on CO_2 capture level at different lean MEA concentrations (55 wt% MEA and 75 wt% MEA). The results show that CO_2 capture level increases significantly from 25 ^{o}C to 50 ^{o}C lean MEA temperatures. When Lean MEA temperature is increased to above 50 ^{o}C, it does not have significant impact on the CO_2 capture level.

Firstly, lean solvent temperature increase leads to dramatic increase in chemical reaction rate. This makes the contact time or resident time required in intensified RPB much smaller compared with conventional technology. Improvement of RPB performance as temperature increases can be also associated to decrease in viscosity of the lean MEA solvent as explain by Lewis and Whitman [30] that the ratio of viscosity to density (kinematic viscosity) of the film fluid is probably the controlling factor in determining film thickness. Haslam *et al.* [31] said that if film resistance is directly proportional to film thickness, then film conductivity is the inverse of kinematic viscosity. The effect of temperature on density of gas is great, but temperature affects the density of lean MEA only slightly [32]. Again an increase in temperature causes an increase in viscosity of a gas but the same increase in temperature might greatly lower the viscosity of lean MEA. This improves mass transfer due to thinner liquid film since absorption of CO_2 into alkanolamines solutions is a liquid film controlled process [26].

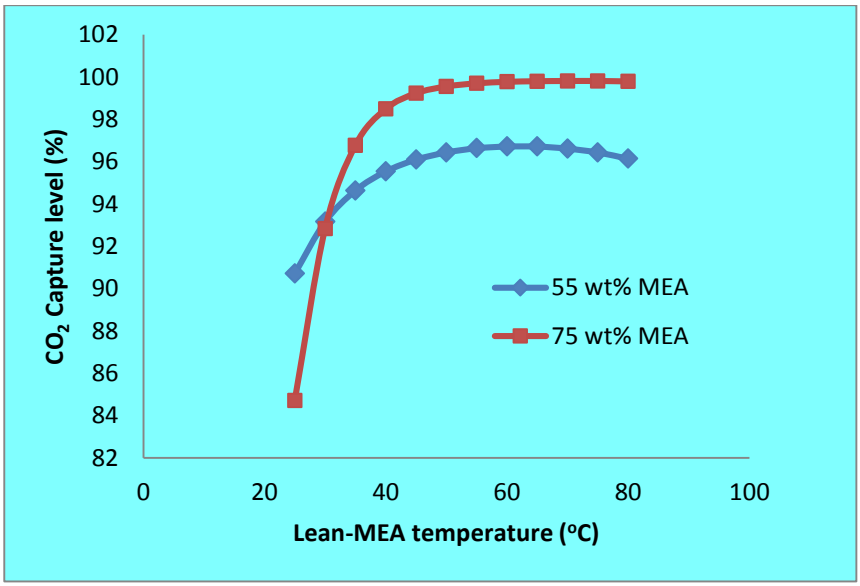

Figure 4 Effect of lean-MEA temperature on CO_2 capture level

3.3 *Effect of Flue Gas Temperature on CO_2 Capture Level*

3.3.1 Justification for case study

Moisture content of a flue gas is dependent on temperature, pressure and the type of fuel used. Study of flue gas temperature is necessary since additional cost will be incurred in cooling flue gas prior to entering conventional absorber [11, 28].

3.3.2 Setup of the case study

Set 2 correlations in Table 1 were used for the formulation of this case study. Run 2 and 4 were selected which are at 56 wt% and 74 wt% MEA concentration respectively. The simulations were run at rotor speed of 1000 rpm, the lean-MEA temperature was kept constant at 40.1 °C for Run 2 and 40.2 °C for Run 4, in both case flue gas temperature was varied from 30 °C to 80 °C.

3.3.3 Results and discussions

Figure 5 show effect of flue gas temperature on CO_2 capture level. The results show that the CO_2 capture level is maintained despite increase in the flue gas temperature. Run 2 and Run 4 give the same trend, this show that even if the solvent is having higher MEA concentration, CO_2 capture level behaves the same way. The reason for this behaviour is because of no temperature bulge as reported in Joel *et al.* [17] since the evaporated vapour condensate does not have enough

residence time for energy build-up in the column. Again because of high liquid to gas (L/G) ratio in an RPB, making the CO_2 capture level not sensitive to the flue gas temperature change. The maintained CO_2 capture level shown in Figure 5 indicates that flue gas cooling energy cost can be saved.

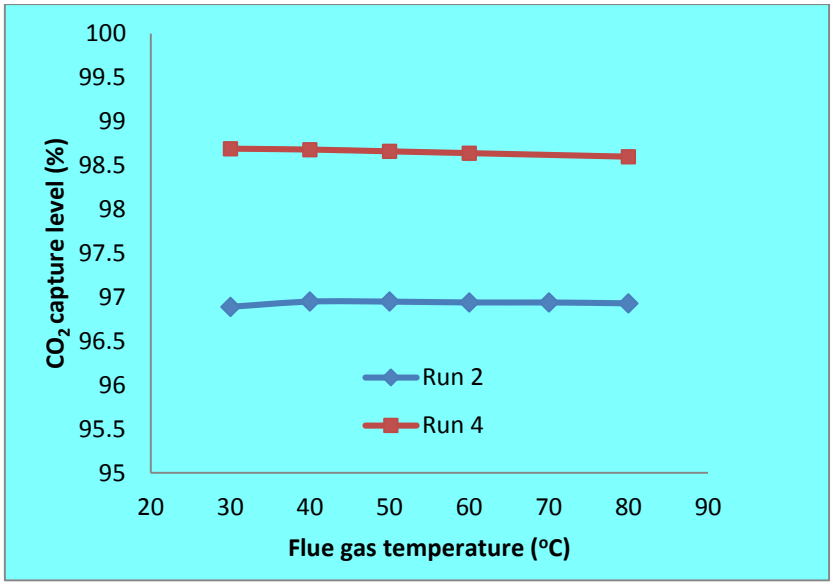

Figure 5 Effect of flue gas temperature on CO_2 capture level

4 Conclusions

Modelling, validation and analysis of a post-combustion CO_2 capture with MEA using intensified absorber was carried out in this paper with two sets of correlations. The RPB absorber was modelled in Aspen Plus(R) which is dynamically linked with visual FORTRAN. Rate-based modelling approach was used and chemical reactions are assumed to be at equilibrium. Experimental data used for validation were obtained from Jassim *et al.* [26].

Two sets of correlations were implemented for the validation of the intensified absorber model and the model predictions showed good agreement with the experimental results. The second set of correlations gives better prediction compared to the first set of correlation. Process was analysed regarding the effect of flue gas flow rate, lean-MEA temperature and flue gas temperature on CO_2 capture level in the intensified absorber. It was found that as the lean-MEA temperature increases the CO_2 capture level increases and as the flue gas temperature increases the CO_2 capture level can be maintained, these mean that cooling duty cost in RPB can be greatly reduced compared with conventional technology. The result shows mass transfer is improved with the use of RPB, also

since the RPB absorber is operated at higher temperature reaction rate is also enhanced.

References

[1] Department of Energy and Climate Change, 2012. *Solid Fuels and Derived Gases Statistics: Data Sources and Methodologies.* Available at: http://www.decc.gov.uk/en/content/cms/statistics/energy_stats/source/coal/coal.aspx (accessed in 05/2012).

[2] J. A. Moulijn, A. Stankiewicz, J. Grievink, A. Go´rak, Process intensification and process systems engineering: a friendly symbiosis. *Comput. Chem. Eng.* 2008, *32* (1-2), 3–11.

[3] Oh, T.H., 2010. Carbon capture and storage potential in coal-fired plant in Malaysia – a review. *Renew. Sust. Energy Rev*. 14, 2697–2709.

[4] Intergovernmental Panel on Climate Change, 2007. Contribution of Working Group III to the Fourth Assessment Report of the Intergovernmental Panel on Climate Change. Cambridge University Press, Cambridge, United Kingdom/New York, United States.

[5] International Energy Agency, 2010. Carbon Capture and Storage Model Regulatory Framework, Available at: http://www.iea.org/ccs/legal/modelframework.pdf (accessed in May 2013).

[6] N. MacDowell, N. Florin, A. Buchard, J. Hallett, A. Galindo, G. Jackson, C.S. Adjiman, C.K. Williams, N. Shah, P. Fennell, An overview of CO_2 capture technologies. Energy and Environmental Science 3 (2010), 1645–1669.

[7] E.R. Dugas. Pilot plant study of carbon dioxide capture by aqueous monoethanolamine. M.S.E. Thesis. University of Texas, Austin, USA. 2006

[8] A. Lawal, M. Wang, P. Stephenson, H. Yeung, Dynamic modelling of CO_2 absorption for post combustion capture in coal-fired power plants. *Fuel* 88 (2009a) 2455–2462

[9] A. Lawal, M. Wang, P. Stephenson, H. Yeung, Dynamic modeling and simulation of CO_2 chemical absorption process for coal-fired power plants. In: de Brito Alves, R.M., Oller do Nascimento, C.A., Chalbaud Biscaia Jr., E. (Eds.), Computer Aided Chemical Engineering. Elsevier, 2009b, 1725–1730.

[10] A. Lawal, M. Wang, P. Stephenson, G. Koumpouras, H. Yeung, Dynamic modelling and analysis of post-combustion CO_2 chemical absorption process for coal-fired power plants. *Fuel* 89 (2010), 2791–2801.

[11] H. M. Kvamsdal, J. P. Jakobsen, K. A. Hoff, Dynamic modeling and simulation of a CO_2 absorber column for post-combustion CO_2 capture. *Chemical Engineering and Processing: Process Intensification* 48(2009), 135-144

[12] D. Reay, The role of process intensification in cutting greenhouse gas emissions. *Applied Thermal Engineering* 28(2008), 2011-2019.

[13] C. Ramshaw, R. H. Mallinson,. Mass transfer process. U.S. Petent, 4*,283,255,* 1981

[14] M. Wang, A. Lawal, P. Stephenson, J. Sidders, C. Ramshaw, Post-combustion CO_2 capture with chemical absorption: A state-of-the-art review. *Chemical Engineering Research and Design* 89(2011), 1609-1624.

[15] BERR, (2006) Advanced power plant using high efficiency boiler/turbine. Report BPB010. BERR, Department for Business Enterprise and Regulatory Reform; Available at: www.berr.gov.uk/files/file30703.pdf. (accessed 04/2012)

[16] A. Lawal, M. Wang, P. Stephenson, O. Obi, Demonstrating full-scale post-combustion CO_2 capture for coal-fired power plants through dynamic modelling and simulation. *Fuel* 101(2012), 115-128.

[17] A. S. Joel, M. Wang, C. Ramshaw, E. Oko, Process analysis of intensified absorber for post-combustion CO_2 capture through modelling and simulation. *International Journal of Greenhouse Gas Control.* Submitted in *June, 2013*

[18] H. H. Tung, R. S. H. Mah, Modeling liquid mass transfer in higee separation process. *Chemical Engineering Communications* 39(1985), 147-153.

[19] K. Onda, E. Sada, H. Takeuchi, Gas absorption with chemical reaction in packed columns. *Journal of Chemical Engineering of Japan,* 1(1968), 62-66.

[20] J. R. Burns, J. N. Jamil, C. Ramshaw, Process intensification: operating characteristics of rotating packed beds — determination of liquid hold-up for a high-voidage structured packing. *Chemical Engineering Science* 55(2000), 2401-2415.

[21] Y. S. Chen, F. Y. Lin, C. C. Lin, C. Y. Tai, H. S Liu, Packing Characteristics for Mass Transfer in a Rotating Packed Bed. *Ind. Eng. Chem. Res. 45(*2006), 6846.

[22] Y. S. Chen, Correlations of Mass Transfer Coefficients in a Rotating Packed Bed. Ind. Eng. Chem. Res., 50(2011), 1778

[23] Y. Luo, G. W. Chu, H. K. Zou, Z. Q. Zhao,M. P. Dudukovic.; J. F. Chen,. Gas – Liquid effective interfacial area in a rotating packed. *Industrial and Engineering Chemistry Research*. 51, (2012), 16320-16325.

[24] C. Biliyok, A. Lawal, M. Wang, F. Seibert, Dynamic modelling, validation and analysis of post-combustion chemical absorption CO_2 capture plant. *International Journal of Greenhouse Gas Control* 9 (2012) 428–445

[25] AspenTech., 2010. Aspen Physical Properties System – Physical Property Methods. Available at: http://support.aspentech.com/ (accessed in May 2012).

[26] M. S. Jassim, G. Rochelle, D. Eimer, C. Ramshaw, Carbon dioxide absorption and desorption in aqueous monoethanolamine solutions in a rotating packed bed. *Industrial & Engineering Chemistry Research* 46(2007), 2823-2833

[27] P. Sandilya, D. P. Rao, A. Sharma, G. Biswas, Gas-Phase Mass Transfer in a Centrifugal Contactor. *Ind. Eng. Chem. Res.*, *40(*2001), 384.

[28] H.M. Kvamsdal, J. Hetland, G. Haugen, H.F. Svendsen, F. Major, V. Kårstad, G. Tjellander, Maintaining a neutral water balance in a 450 MWe NGCC-CCS power system with post-combustion carbon dioxide capture aimed at offshore operation. International Journal of Greenhouse Gas Control 4 (2010), 613–622.

[29] S. Freguia, G.T. Rochelle, Modeling of CO_2 capture by aqueous monoethanolamine. *AIChE Journal* 49 (2003), 1676–1686.

[30] W. K. Lewis, W. G. Whitman, Principles of gas absorption. *Industrial and Engineering Chemistry* 16(1924), 1215-1220.

[31] R. T. Haslam, Hershey, R. L., Keen, R. H.,. Effect of gas velocity and temperature on rate of absorption. *Industrial and Engineering Chemistry* 16(1924), 1224-1230.

[32] R. Maceiras, E. Álvarez, M.Á. Cancela, Effect of temperature on carbon dioxide absorption in monoethanolamine solutions. *Chemical Engineering Journal,* 138(2008), pp. 295-300